Inorganic Chemistry

Article

pubs.acs.org/IC

Crystal Structure and Microwave Dielectric Behaviors of Ultra-Low-Temperature Fired $x(Ag_{0.5}Bi_{0.5})MoO_4-(1-x)BiVO_4$ ($0.0 \leq x \leq 1.0$) Solid Solution with Scheelite Structure

Di Zhou,*[,†] Li-Xia Pang,[‡] and Ze-Ming Qi[§]

[†]Electronic Materials Research Laboratory, Key Laboratory of the Ministry of Education & International Center for Dielectric Research, Xi'an Jiaotong University, Xi'an 710049 Shaanxi, People's Republic of China

[‡]Micro-optoelectronic Systems Laboratories, Xi'an Technological University, Xi'an 710032, Shaanxi, People's Republic of China

[§]National Synchrotron Radiation Laboratory, University of Science and Technology of China, Hefei 230029, Anhui, People's Republic of China

ABSTRACT: $x(Ag_{0.5}Bi_{0.5})MoO_4-(1-x)BiVO_4$ ($0.0 \leq x \leq 1.0$) ceramics were prepared by using the solid-state reaction technique. Ceramics with $x < 0.10$ had a monoclinic scheelite structure, while those with ≥ 0.10 were tetragonal scheelite solid solutions. This indicates that the phase transformation temperature of $BiVO_4$ was lowered through the formation of a solid solution. The thermal expansion data of the $x = 0.08$ sample showed that the thermal expansion coefficient was increased suddenly from +8 to +15 ppm/°C at about 60.6 °C due to the phase transition. Similarly, a maximum value of microwave dielectric permittivity was revealed at about 65 °C for the $x = 0.08$ sample. All of the ceramics could be well sintered below 700 °C. Good microwave dielectric behaviors, with relative permittivity >75 and $Q_f > 9000$ GHz, were obtained in ceramics with compositions near $x = 0.10$. Both the THz data and the infrared spectra were used to study the intrinsic dielectric behavior of the materials at microwave frequencies.

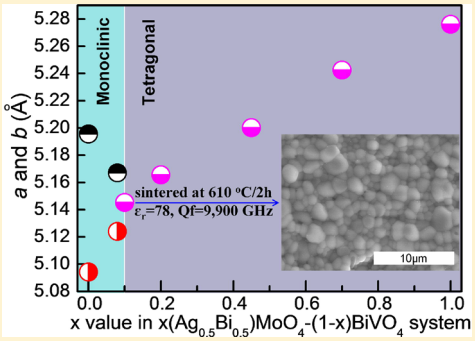

INTRODUCTION

Microwave dielectric ceramics have played a key role in advancing modern radio communication technology. The search for novel microwave dielectric systems with ultralow dielectric loss (high quality factor Q_f) and appropriate dielectric permittivities has always been a hot topic.[1,2] Due to the requirement of high integration, miniaturization, and reliability for microwave devices, low-temperature cofired ceramics (LTCC) technology has become a irreplaceable fabrication method.[3,4] In addition to the high quality factor, the ceramics are required to have sintering temperatures lower than the melting point of the inner metal electrode. Addition of sintering frits is the traditional method to lower densification temperatures of microwave ceramics.[3−6] However, the presence of sintering frits usually deteriorates the quality factor of microwave dielectric ceramics. In the past decade, microwave ceramics with intrinsic low dielectric loss have attracted a great deal of attention; TeO_2-rich and MoO_3-rich systems have been explored.[7,8]

$BiVO_4$ has been studied widely for use in pigments, high-temperature conductors, and dielectrics and as a photocatalyst.[9−14] As reported by Valant and Wee et al., monoclinic scheelite structured $BiVO_4$ ceramic possessed good microwave dielectric properties, with $\varepsilon_r \approx 68$, $Q_f \approx 7000$ GHz, a temperature coefficient of resonant frequency (TCF or τ_f) of ∼−250 ppm/°C, and a sintering temperature below 900 °C.[14,15] In our previous work,[16−18] it was found that complex substitution at the A and B sites with alkali-metal (Li^+, Na^+, K^+) and bismuth (Bi^{3+}) ions, respectively, can result in the formation of scheelite structured solid solutions with improved microwave dielectric properties and modified sintering temperatures. In addition, the monoclinic scheelite solid solution can effectively extend the band gap to a range of 2.20−2.35 eV, which makes it a potential photocatalyst for water splitting under visible irradiation.[19] Also, Ag^+ was found to enter the A site of the ABO_4 scheelite structure, combined with Bi^{3+} ion to form $(Ag_{0.5}Bi_{0.5})MoO_4$, which was reported to be sintered at 690 °C, with promising microwave dielectric behaviors,: i.e., a relative permittivity ∼30.4, a Q_f value of ∼12600 GHz, and a TCF value of +57 ppm/°C.[20,21] In the present work, the $x(Ag_{0.5}Bi_{0.5})MoO_4-(1-x)BiVO_4$ ceramics were synthesized through the solid-state reaction technique, to study sintering behavior, phase composition, microwave dielectric behavior, and the structure−property relation.

EXPERIMENTAL SECTION

Reagent-grade starting materials of Ag_2CO_3, Bi_2O_3, V_2O_5 (>99%, Sinopharm Chemical Reagent Co., Ltd., Shanghai, People's Republic of China), and MoO_3 (>99%, Fuchen Chemical Reagents, Tianjin, People's Republic of China) were mixed according to the

Received: June 6, 2014
Published: August 8, 2014

   dx.doi.org/10.1021/ic501306n | Inorg. Chem. 2014, 53, 9222−9227

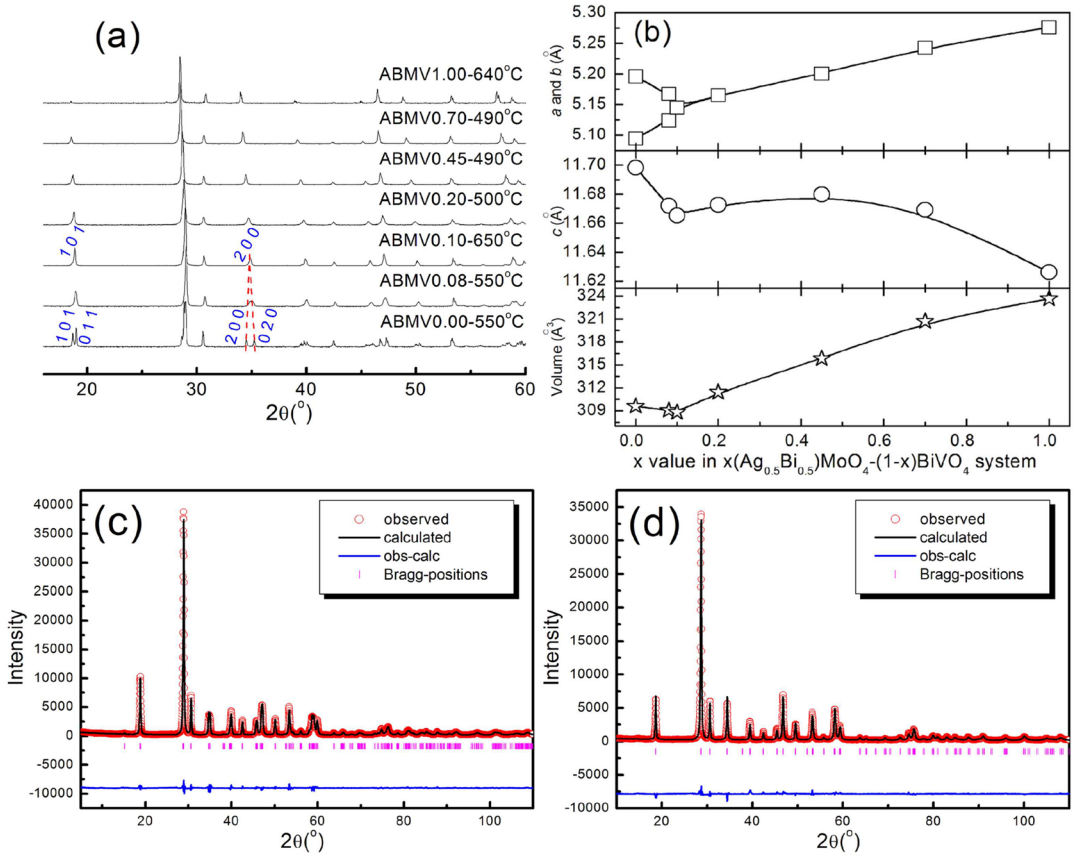

Figure 1. (a) XRD patterns of the $x(Ag_{0.5}Bi_{0.5})MoO_4-(1-x)BiVO_4$ ($0.0 \le x \le 1.0$) ceramics calcined at different temperatures, (b) cell parameters as a function of x, and experimental (circles) and calculated (line) X-ray powder diffraction profiles for the (c) $x = 0.08$ and (d) $x = 0.45$ samples at room temperature ($R_p = 8.71$, $R_{wp} = 10.4$, and $R_{exp} = 5.17$ for $x = 0.08$ sample; $R_p = 11.0$, $R_{wp} = 12.6$, and $R_{exp} = 5.85$ for $x = 0.45$ sample). For parts c and d, the short vertical lines below the patterns mark the positions of Bragg reflections. The bottom continuous line is the difference between the observed and calculated intensities.

stoichiometric formulations $x(Ag_{0.5}Bi_{0.5})MoO_4-(1-x)BiVO_4$ ($0.0 \le x \le 1.0$), by ball milling for 4 h using a planetary mill machine (Nanjing Machine Factory, Nanjing, People's Republic of China) at 150 rpm, with zirconia balls (2 mm in diameter) as milling media. Then the mixtures were rapidly dried and calcined at 490−600 °C for 4 h, depending on composition. Powders after calcinations were ball-milled again for 5 h at 200 rpm. Subsequently, 5 wt % of PVA was added to the powders and the mixtures were pressed into cylindrical samples (about 10 mm in diameter and 4 mm in height) with a steel die at a uniaxial pressure of 100 MPa. Green samples were finally sintered at temperatures from 510 to 650 °C for 2 h in air.

Room-temperature X-ray diffraction (XRD) was performed with Cu Kα radiation (Rigaku D/MAX-2400 X-ray diffractometry, Tokyo, Japan). Prior to examination, the sintered pellets were crushed with a mortar to powder. The diffraction pattern was obtained over 10−60° at a step of 0.02°. The data were performed by the Rietveld profile refinement method, using the FULLPROF program. To examine grain morphology, as-fired surfaces were observed by using scanning electron microscopy (SEM) (ESEM, FEI, Quanta 200). Room-temperature infrared reflectivity spectra were obtained by using a FTIR spectrometer (Bruker IFS 66v, Germany) on the infrared beamline station (U4) at the National Synchrotron Radiation Laboratory (NSRL) of the People's Republic of China. Dielectric behaviors at terahertz frequencies from 0.09 to 0.85 THz (2.8−28 cm^{-1}) were measured by using terahertz time-domain (THz TDS) spectroscopy (ADVAVTEST TAS7500SP, Japan). A passive mode-lock fiber laser was used to pump and gate respectively two GaAs photoconductive antennas for the generation and detection of THz waves. Microwave dielectric behaviors were obtained by using the $TE_{01\delta}$ resonator method employing a network analyzer (HP 8720 Network Analyzer, Agilent) and a programmable chamber (Delta 9023, Delta Design, Poway, CA). The τ_f value was calculated by the formula

$$\mathrm{TCF}\ (\tau_f) = \frac{f_T - f_{T_0}}{f_{T_0} \times (T - T_0)} \times 10^6 \quad (1)$$

where f_T and f_{T_0} are the $TE_{01\delta}$ resonant frequencies at temperatures T and T_0, respectively.

RESULTS AND DISCUSSION

XRD patterns of the $x(Ag_{0.5}Bi_{0.5})MoO_4-(1-x)BiVO_4$ ceramics, which were calcined over 490−650 °C, are presented in Figure 1a. It is found that a full scheelite structured solid solution was obtained, which is similar to our previous work on $x(Li_{0.5}Bi_{0.5})MoO_4-(1-x)BiVO_4$ and $x(Na_{0.5}Bi_{0.5})MoO_4-(1-x)BiVO_4$ systems.[22,17] As x is increased from 0.0 to 0.1, a merging of characteristic reflection peaks, such as (011) and (101) peaks into a (101) peak, is clearly observed, which results from the continuous ferroelastic phase transition (monoclinic → tetragonal structure). Figure 1b presents the cell parameters and cell volume of the $x(Ag_{0.5}Bi_{0.5})MoO_4-(1-x)BiVO_4$ compositions as a function of x value. In the scheelite structure, ionic radii of eight-coordinated Ag^+ and Bi^{3+} are 1.28 and 1.17 Å, respectively, while those of four-coordinated Mo^{6+} and V^{5+} are 0.41 and 0.355 Å, respectively, as reported by Shannon.[23] It can be observed that a decreases and b increases with increasing x value. They become closer and closer and finally develop into the same value, which indicates that the crystalline structure

dx.doi.org/10.1021/ic501306n | Inorg. Chem. 2014, 53, 9222−9227

was changed to a tetragonal phase. Meanwhile, c is also decreased, this resulting in a decrease in cell volume. This phase transition was believed to be induced by the internal pressure caused by the ionic radius of Mo^{6+} being larger than that of V^{5+} at the B site.[17,22] As x reaches 0.10, although c value is decreased slightly, the increase in a (or b) resulted in an increase in cell volume (cell volume = $a^2 \times c$). The increase in a was ascribed to the ionic radius of Ag^+ being larger than that of Bi^{3+}.

To study the details of crystal structures with Ag and Mo substitution, structure refinements were performed on the x = 0.08 and x = 0.45 samples. The calculated and measured XRD patterns are presented in Figure 1c,d. The refined values of lattice parameters of the x = 0.08 sample are a = 5.1675(2) Å, b = 5.1247(7) Å, c = 11.6721(6) Å, and γ = 90.120(3)°, with the space group $I1_12/b$ (No. 15), according to Sleight et al.'s data (ICSD #100602).[24] The refined lattice parameters of the x = 0.45 sample are $a = b$ = 5.204906 Å and c = 11.672254 Å, with a space group $I4_1/a$ (No. 88), using Hanuza et al.'s data (ICSD #100602).[25] The details of cell parameters are given in Tables 1

Table 1. Refined Atomic Fractional Coordinates from XRD Data for the x = 0.08 Sample[a]

atom	site	occ	x	y	z	B_{iso}
Ag	4e	0.02	0.00000	0.25000	0.62928	0.74238
Bi	4e	0.48	0.00000	0.25000	0.62928	0.74238
Mo	4e	0.04	0.00000	0.25000	0.12877	0.37894
V	4e	0.46	0.00000	0.25000	0.12877	0.37894
O1	8f	1.00	0.14375	0.48672	0.21066	0.78477
O2	8f	1.00	0.25181	0.39069	0.44754	0.81289

[a]The lattice parameters at room temperature are a = 5.1675(2) Å, b = 5.1247(7) Å, c = 11.6721(6) Å, and γ = 90.120(3)°. The space group is $I1_12/b$ (No. 15).

Table 2. Refined Atomic Fractional Coordinates from XRD Data for the x = 0.45 Sample[a]

atom	site	occ	x	y	z	B_{iso}
Ag	4b	0.1125	0.00000	0.25000	0.62500	0.93881
Bi	4b	0.3875	0.00000	0.25000	0.62500	0.93881
Mo	4a	0.225	0.00000	0.25000	0.12500	0.70352
V	4a	0.275	0.00000	0.25000	0.12500	0.70352
O	16f	1.00	0.16287	0.02554	0.21085	1.32567

[a]The lattice parameters at room temperature are $a = b$ = 5.204906 Å and c = 11.672254 Å. The space group is $I4_1/a$ (No. 88).

and 2. In the monoclinic structure, there are two types of B−O bonds. The average long and short B−O distances of the x = 0.08 sample are 1.739 and 1.671 Å, respectively, and both are shorter than those of $BiVO_4$ (1.767 and 1.692 Å, respectively). At the same time, the (Bi,Ag)−O distances (2.429 and 2.401 Å) in the x = 0.08 sample are longer than those of $BiVO_4$ (2.372 and 2.354 Å). The (Bi,Ag)−O and (Mo,V) bond distances in the x = 0.45 sample are 2.478 and 1.757 Å, respectively, which are longer than those of $BiVO_4$. The substitution of Ag and Mo effectively increased the cell volume.

As reported in our previous work, a thermal expansion experiment is an effective tool to identify the phase transition temperature, rather than differential thermal analysis, in the case of a second-order phase transformation.[26] The thermal expansion curve of the $x(Ag_{0.5}Bi_{0.5})MoO_4-(1-x)BiVO_4$ (x = 0.08) sample as a function of temperature is presented in Figure 2. It is found that the thermal expansion rate suddenly

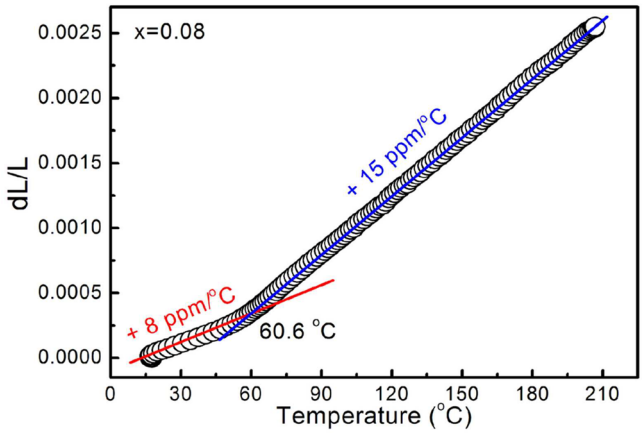

Figure 2. Thermal expansion data of the $x(Ag_{0.5}Bi_{0.5})MoO_4-(1-x)BiVO_4$ (x = 0.08) ceramics as a function of temperature.

increased at the temperature was increased above 60.6 °C, along with the coefficient of thermal expansion shifting from +15 to +8 ppm/°C, and this is similar to the results for pure $BiVO_4$.

Surface SEM images of the $x(Ag_{0.5}Bi_{0.5})MoO_4-(1-x)BiVO_4$ ceramics (x = 0.10, 0.20, 0.45, 0.70) sintered at their optimal sintering temperatures are presented in Figure 3.

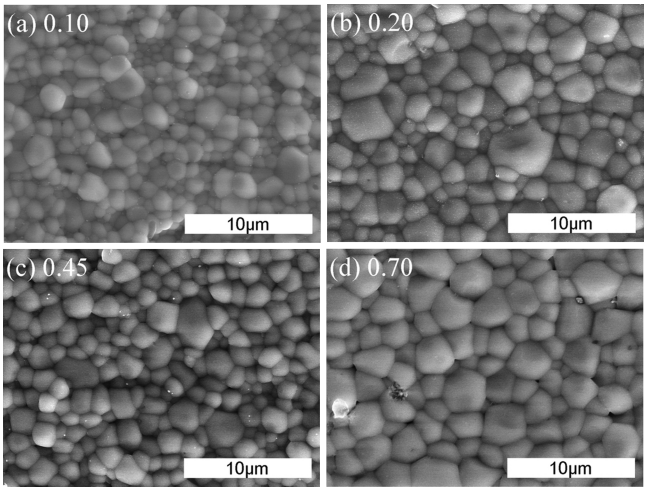

Figure 3. SEM photos of the $x(Ag_{0.5}Bi_{0.5})MoO_4-(1-x)BiVO_4$ ceramics: (a) x = 0.10 sintered at 610 °C; (b) x = 0.20 sintered at 610 °C; (c) x = 0.45 sintered at 530 °C; (d) x = 0.70 sintered at 530 °C.

Homogeneity and densification of microstructures were achieved in all ceramics. The grain size increases slightly from 1−2 μm at x = 0.10 to 2−3 μm at x = 0.70. It is found that formation of the solid solution effectively lowered the densification temperature of the $x(Ag_{0.5}Bi_{0.5})MoO_4-(1-x)BiVO_4$ ceramics to about 530 °C at x = 0.45, which is much lower than those of both pure $BiVO_4$ and $(Ag_{0.5}Bi_{0.5})MoO_4$ ceramics (800 and 690 °C). This observation is similar to that in the $Bi(Sb_{1-x}Ta_x)O_4$ system.

dx.doi.org/10.1021/ic501306n | Inorg. Chem. 2014, 53, 9222−9227

Microwave dielectric behaviors of the $x(Ag_{0.5}Bi_{0.5})MoO_4-(1-x)BiVO_4$ ($0.0 \le x \le 1.0$) ceramics at room temperature are plotted in Figure 4 as a function of x value (4–9 GHz). The

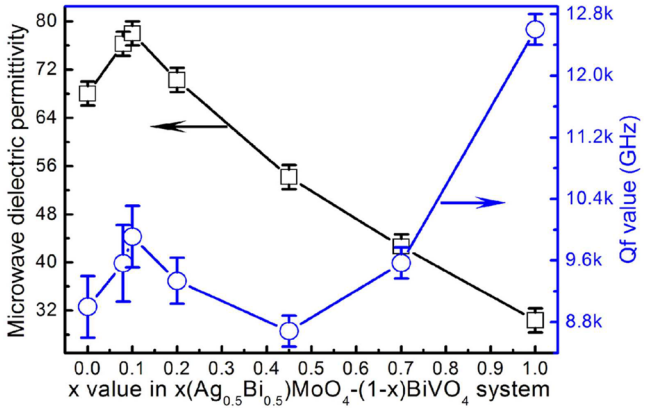

Figure 4. Room-temperature microwave dielectric properties of the $x(Ag_{0.5}Bi_{0.5})MoO_4-(1-x)BiVO_4$ ($0.0 \le x \le 1.0$) ceramics as a function of x.

relative permittivity linearly increased from 68 for $BiVO_4$ to a maximum value of about 78 at $x = 0.10$. Then it decreased sharply to 30.4 for $(Ag_{0.5}Bi_{0.5})MoO_4$. The peak value of permittivity was obtained for a composition near the phase boundary between the monoclinic and tetragonal scheelite phases, and this should be ascribed to the minimal cell volume at this point. The continuous decrease of relative permittivity in the tetragonal structured region was ascribed to a decrease in the equivalent ionic polarizability[27] ($\alpha = 0.5x\alpha_{Ag^+} + (1-0.5x)\alpha_{Bi^{3+}} + x\alpha_{Mo^{6+}} + (1-x)\alpha_{V^{5+}} + 4\alpha_{O^{2-}}$, about $17.08 - 1.575x$ Å^3) and the increase in the cell volume, as discussed above. Q_f values of $x(Ag_{0.5}Bi_{0.5})MoO_4-(1-x)BiVO_4$ ceramics increased from 8900 GHz for pure $BiVO_4$ to about 10500 GHz for an $x = 0.10$ sample (at 4.6 GHz) and then decreased to a minimum value of 8680 GHz at $x = 0.45$ (5.2 GHz). With a further increase of x, the Q_f value increased linearly to about 12600 GHz for $(Ag_{0.5}Bi_{0.5})MoO_4$ (8.7 GHz).

The temperature stabilities of microwave dielectric behaviors of the $x(Ag_{0.5}Bi_{0.5})MoO_4-(1-x)BiVO_4$ ceramics are presented in Figure 5. There will be a peak value of permittivity in the case of phase transformation coupled to an optical mode on the basis of the Lyddane–Sachs–Teller (LST) relation.[28] A peak value of microwave dielectric permittivity of the $x = 0.08$ sample can be observed at about 65 °C, which corresponds well with the thermal expansion analysis. When the x value is larger than 0.10, all of the $x(Ag_{0.5}Bi_{0.5})MoO_4-(1-x)BiVO_4$ ceramics are in the tetragonal phase, so that there is no abnormality observed in the relative permittivity curves and the relative permittivities decrease linearly with temperature, with the TCF value shifting from +198 ppm/°C at $x = 0.10$ to +73 ppm/°C. The Q_f value of the $x = 0.08$ sample decreased sharply from 9200 GHz at 25 °C to below 5000 GHz at 140 °C. For samples with $x \ge 0.10$, Q_f values only decreased slightly with temperature, which indicates that the formation of the solid solution increased the temperature stability.

IR reflectance spectra of the $x(Ag_{0.5}Bi_{0.5})MoO_4-(1-x)BiVO_4$ ($x = 0.20$, 0.45 and 0.70) samples were analyzed with the classical harmonic oscillator model:

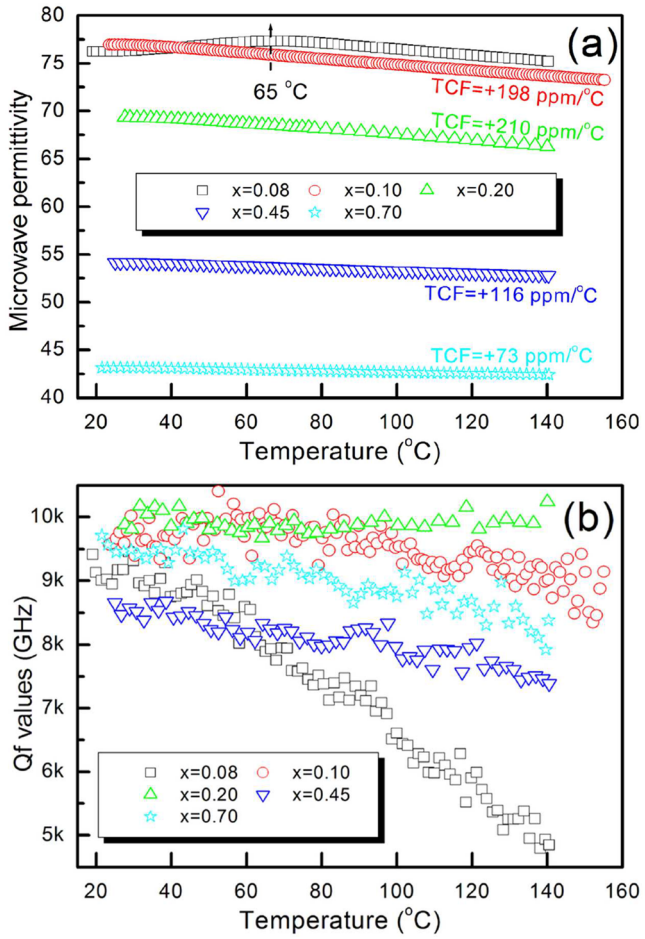

Figure 5. Microwave dielectric permittivity (a) and Q_f values (b) of $x(Ag_{0.5}Bi_{0.5})MoO_4-(1-x)BiVO_4$ ($0.0 \le x \le 1.0$) ceramics as a function of temperature.

$$\varepsilon^*(\omega) = \varepsilon_\infty + \sum_{j=1}^{n} \frac{\omega_{pj}^2}{\omega_{oj}^2 - \omega^2 - j\gamma_j\omega} \quad (2)$$

where $\varepsilon^*(\omega)$ is complex dielectric constant, ε_∞ is the optical dielectric constant, and γ_j, ω_{oj}, and ω_{pj} are the damping coefficient, transverse frequency, and plasma frequency of the jth Lorentz oscillator, respectively. Then the complex reflectance $R(\omega)$ is related by

$$R(\omega) = \left| \frac{1 - \sqrt{\varepsilon^*(\omega)}}{1 + \sqrt{\varepsilon^*(\omega)}} \right|^2 \quad (3)$$

Fitted IR reflectance values and complex dielectric constant are presented in Figures 6 and 7, respectively. Phonon parameters obtained from the fitting of the infrared reflectivity spectra of $x(Ag_{0.5}Bi_{0.5})MoO_4$-$(1-x)BiVO_4$ ($x = 0.20$, 0.70) ceramics are given in Table 3. It is found that calculated and measured values (dielectric permittivity and loss) agree well with each other and this indicates that dielectric polarization for $x(Ag_{0.5}Bi_{0.5})$-$MoO_4-(1-x)BiVO_4$ ceramics at microwave frequency is dominated by the phonon oscillation at far-infrared frequency range. It is found that the contributions of dielectric polarization from the two vibration bands below 160 cm^{-1} run up to 87% for both the $x = 0.20$ and $x = 0.70$ samples. This confirms that dielectric polarization contributions in bismuth-based scheelite solid solution are mainly contributed by external

dx.doi.org/10.1021/ic501306n | Inorg. Chem. 2014, 53, 9222–9227

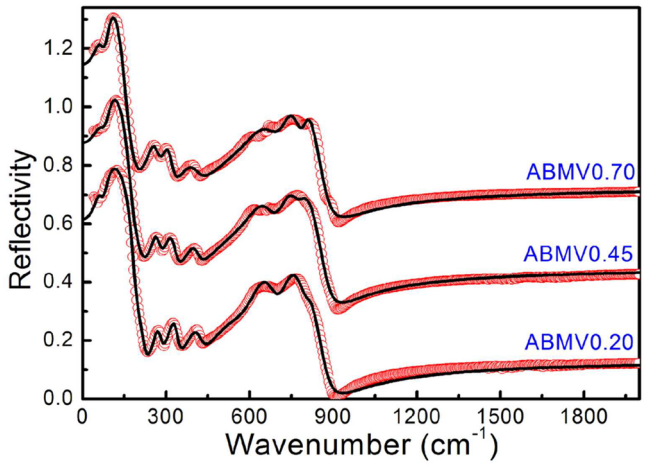

Figure 6. Measured and calculated infrared reflectivity spectra of the $x(Ag_{0.5}Bi_{0.5})MoO_4-(1-x)BiVO_4$ (x = 0.20, 0.45 and 0.70) ceramics (solid line for fitted values and circles for measured values).

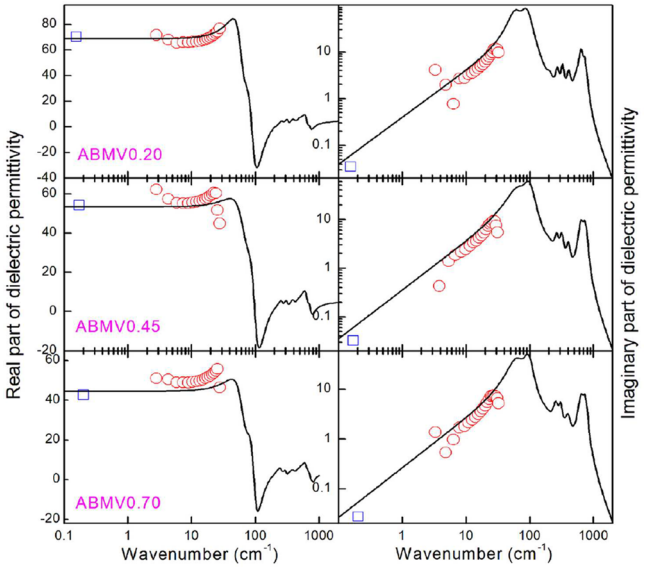

Figure 7. Complex dielectric spectra of the $x(Ag_{0.5}Bi_{0.5})MoO_4-(1-x)BiVO_4$ (x = 0.20, 0.45, 0.70) ceramics (circles are experimental values in the microwave region and THz data, and solid lines represent the fit of IR spectra).

bands (Bi−O stretches)[29] and the Bi^{3+} ions, accounting for the microwave dielectric permittivity being larger than that of the $(Ba,Sr,Ca)(Mo,W)O_4$ system.[30]

CONCLUSIONS

Scheelite structured solid solutions $x(Ag_{0.5}Bi_{0.5})MoO_4-(1-x)BiVO_4$ ceramics can be synthesized by using the solid-state reaction technique. The phase transformation monoclinic → tetragonal structure was clearly observed in compositions near x = 0.10, which indicates that the transformation temperature was decreased from 255 °C for $BiVO_4$ to near 25 °C at x = 0.10, which was supported by thermal expansion data and the dielectric spectra at microwave frequency. All of the ceramics were well sintered at temperatures <700 °C. Sample with x = 0.45 can be sintered at as low as 530 °C. Promising microwave dielectric behaviors, with relative permittivities >75 and Q_f values >9000 GHz, were obtained in samples with compositions near x = 0.10. The majority of the dielectric polarization at microwave frequency was contributed by the phonon oscillation, which was proved by both the THz data and the fit of IR spectra. This system is promising for application in microwave devices with LTCC technology.

AUTHOR INFORMATION

Corresponding Author

*D.Z.: tel (fax), +86-29-82668679; e-mail, zhoudi1220@gmail.com.

Notes

The authors declare no competing financial interest.

ACKNOWLEDGMENTS

This work was supported by the National Natural Science Foundation of China (51202182, 51202178, 61371035), National Key Scientific Instrument and Equipment Development Project (2011YQ130018), the Fundamental Research Funds for the Central University, the International Cooperation Project of Shaanxi Province (2013KW12-04), the State Key Laboratory of New Ceramic and Fine Processingm, Tsinghua University, and the 111 Project of China (B14040). The authors would like to thank the administrators of the IR beamline workstation of National Synchrotron Radiation Laboratory (NSRL) for their help in the IR measurements. SEM work was partially done at the International Center for Dielectric Research (ICDR), Xi'an Jiaotong University, Xi'an, People's Republic of China, and the authors thank Ms. Yan-Zhu Dai for her help in using SEM. The authors thank Prof. Dr. Jin

Table 3. Phonon Parameters Obtained from the Fitting of the Infrared Reflectivity Spectra of $x(Ag_{0.5}Bi_{0.5})MoO_4-(1-x)BiVO_4$ (x = 0.20, 0.70) Ceramics[a]

mode	ω_{oj}	ω_{pj}	γ_j	$\Delta\varepsilon_j$	mode	ω_{oj}	ω_{pj}	γ_j	$\Delta\varepsilon_j$
1	60.56	322.77	30.99	28.4	1	63.82	287.52	40.22	20.3
2	89.94	505.69	39.57	31.6	2	95.47	371.78	34.78	15.2
3	206.47	113.42	46.75	0.30	3	181.89	168.74	100.37	0.86
4	271.07	172.1	32.26	0.40	4	257.44	226.25	51.52	0.77
5	328.11	230.69	39.65	0.49	5	305.94	210.60	41.79	0.47
6	411.39	270.68	61.73	0.43	6	397.82	278.89	89.66	0.49
7	541.24	304.53	116.68	0.32	7				
8	641.13	813.03	101.53	1.61	8	649.51	791.43	138.24	1.48
9	731.01	575.32	87.81	0.62	9	734.04	555.12	82.92	0.57
10	806.62	159.33	54.56	0.04	10	797.43	262.91	49.34	0.11

[a] x = 0.20: ε_∞ = 4.56 and ε_0 = 68.77. x = 0.70: ε_∞ = 4.34 and ε_0 = 40.26.

dx.doi.org/10.1021/ic501306n | Inorg. Chem. 2014, 53, 9222−9227

(Biao-Bing Jin) from Nanjing University for his help in the terahertz spectroscopy measurements.

REFERENCES

(1) Mirsaneh, M.; Leisten, O. P.; Zalinska, B.; Reaney, I. M. *Adv. Funct. Mater.* **2008**, *18*, 2293−2300.
(2) Chu, L. W.; Hsiue, G. H.; Lin, I. N. *Acta Mater.* **2006**, *54*, 1671−1677.
(3) Sebastian, M. T.; Jantunen, H. *Int. Mater. Rev.* **2008**, *53*, 57−90.
(4) Axelsson, A. K.; Alford, N. M. *J. Eur. Ceram. Soc.* **2006**, *26*, 1933−1936.
(5) Pang, L. X.; Wang, H.; Zhou, D.; Yao, X. *J. Mater. Sci. Mater. Electron.* **2010**, *21*, 1285−1292.
(6) Zhou, D.; Randall, C. A.; Pang, L. X.; Wang, H.; Wu, X. G.; Guo, J.; Zhang, G. Q.; Shui, L.; Yao, X. *J. Am. Ceram. Soc.* **2011**, *94*, 802−5.
(7) Kwon, D. K.; Lanagan, M. T.; Shrout, T. R. *J. Am. Ceram. Soc.* **2005**, *88*, 3419−3422.
(8) Zhou, D.; Wang, H.; Yao, X.; Pang, L. X. *J. Am. Ceram. Soc.* **2008**, *91*, 3419−3422.
(9) Duraisamy, T.; Ramanan, A. *Solid State Ionics* **1999**, *120*, 233−237.
(10) Bierlein, J. D.; Sleight, A. W. *Solid State Commun.* **1975**, *16*, 69−70.
(11) Li, G. S.; Zhang, D. Q.; Yu, J. C. *Chem. Mater.* **2008**, *20*, 3983−3992.
(12) David, W. I. F.; Glazer, A. M.; Hewat, A. W. *Phase Transitions* **1979**, *1*, 155−169.
(13) Pinczuk, A.; Welber, B.; Dacol, F. H. *Solid State Commun.* **1979**, *29*, 515−518.
(14) Wee, S. H.; Kim, D. W.; Yoo, S. I. *J. Am. Ceram. Soc.* **2004**, *87*, 871−874.
(15) Valant, M.; Suvorov, D. *J. Am. Ceram. Soc.* **2000**, *83*, 2721−2729.
(16) Zhou, D.; Randall, C. A.; Wang, H.; Pang, L. X.; Yao, X. *J. Am. Ceram. Soc.* **2010**, *93*, 2147−2150.
(17) Zhou, D.; Pang, L. X.; Wang, H.; Guo, J.; Yao, X.; Randall, C. A. *J. Mater. Chem.* **2011**, *21*, 18412−18420.
(18) Zhou, D.; Pang, L. X.; Guo, J.; Wang, H.; Yao, X.; Randall, C. A. *Inorg. Chem.* **2011**, *50*, 12733−12738.
(19) Zhou, D.; Pang, L. X.; Qu, W. G.; Randall, C. A.; Guo, J.; Qi, Z. M.; Shao, T.; Yao, X. *RSC Adv.* **2013**, *3*, 5009−5014.
(20) Perepelitsa, A. *Russ. J. Inorg. Chem.* **1977**, *22*, 549.
(21) Zhou, D.; Randall, C. A.; Pang, L. X.; Wang, H.; Guo, J.; Zhang, G. Q.; Wu, Y.; Guo, K. T.; Shui, L.; Yao, X. *Mater. Chem. Phys.* **2011**, *129*, 688−692.
(22) Zhou, D.; Qu, W. G.; Randall, C. A.; Pang, L. X.; Wang, H.; Wu, X. G.; Guo, J.; Zhang, G. Q.; Shui, L.; Wang, Q. P.; Liu, H. C.; Yao, X. *Acta Mater.* **2011**, *59*, 1502−1509.
(23) Shannon, R. D. *Acta Crystallogr., Sect. A* **1976**, *A32*, 751−767.
(24) Sleight, A. W.; Chen, H. Y.; Ferretti, A.; Cox, D. E. *Mater. Res. Bull.* **1979**, *14*, 1571−1581.
(25) Hanuza, J.; Haznar, A.; Maczka, M.; Pietraszko, A.; Lemiec, A.; van der Maas, J. H.; Lutz, E. T. G. *J. Raman Spectrosc.* **1997**, *28*, 953−963.
(26) Zhou, D.; Pang, L. X.; Guo, J.; Qi, Z. M.; Shao, T.; Yao, X.; Randall, C. A. *J. Mater. Chem.* **2012**, *22*, 21412−21419.
(27) Shannon, R. D. *J. Appl. Phys.* **1993**, *73*, 348−366.
(28) Lyddane, R. H.; Sachs, H.; Tellar, E. *Phys. Rev.* **1941**, *59*, 673−676.
(29) Zhou, D.; Li, W. B.; Pang, L. X.; Guo, J.; Qi, Z. M.; Shao, T.; Yao, X.; Randall, C. A. *Dalton Trans.* **2014**, *43*, 7290−7297.
(30) Choi, G. K.; Kim, J. R.; Yoon, S. H.; Hong, K. S. *J. Eur. Ceram. Soc.* **2007**, *27*, 3063−3067.